



HAL
open science

Direct synthesis of mesoporous silica containing cobalt: A new strategy using a cobalt soap as a co-template

Sarah Grosshans-Vières, Fanny Tihay-Schweyer, Pierre Rabu, Jean-Louis Paillaud, Pierre Braunstein, Bénédicte Lebeau, Claude Estournès, J.-L. Guille, Jean-Michel Rueff

► **To cite this version:**

Sarah Grosshans-Vières, Fanny Tihay-Schweyer, Pierre Rabu, Jean-Louis Paillaud, Pierre Braunstein, et al.. Direct synthesis of mesoporous silica containing cobalt: A new strategy using a cobalt soap as a co-template. *Microporous and Mesoporous Materials*, 2007, 106 (1 - 3), pp.17-27. 10.1016/j.micromeso.2007.01.056 . hal-03592608

HAL Id: hal-03592608

<https://hal.science/hal-03592608>

Submitted on 1 Mar 2022

HAL is a multi-disciplinary open access archive for the deposit and dissemination of scientific research documents, whether they are published or not. The documents may come from teaching and research institutions in France or abroad, or from public or private research centers.

L'archive ouverte pluridisciplinaire **HAL**, est destinée au dépôt et à la diffusion de documents scientifiques de niveau recherche, publiés ou non, émanant des établissements d'enseignement et de recherche français ou étrangers, des laboratoires publics ou privés.



Open Archive Toulouse Archive Ouverte (OATAO)

OATAO is an open access repository that collects the work of Toulouse researchers and makes it freely available over the web where possible.

This is an author-deposited version published in: <http://oatao.univ-toulouse.fr/>
Eprints ID : 2474

To link to this article :

URL : <http://dx.doi.org/10.1016/j.micromeso.2007.01.056>

To cite this version : Grosshans-Vières, S. and Tihay-Schweyer, F. and Rabu, Pierre and Paillaud, Jean-Louis and Braunstein, P. and Lebeau, B. and Estournès, Claude and Guille, J.-L. and Rueff, J.-M. (2007) [*Direct synthesis of mesoporous silica containing cobalt: A new strategy using a cobalt soap as a co-template.*](#) Microporous and Mesoporous Materials, vol. 106 (n° 1 - 3). pp. 17-27. ISSN 1387-1811

Any correspondence concerning this service should be sent to the repository administrator: staff-oatao@inp-toulouse.fr

Direct synthesis of mesoporous silica containing cobalt: A new strategy using a cobalt soap as a co-template

S. Grosshans-Vières^{a,b,c}, F. Tihay-Schweyer^{a,b,c}, P. Rabu^{b,d,*}, J.-L. Paillaud^{a,*}, P. Braunstein^{c,*}, B. Lebeau^a, C. Estournès^{b,1}, J.-L. Guille^b, J.-M. Rueff^b

^a *Laboratoire de Matériaux à Porosité Contrôlée, UMR 7016 CNRS, Ecole Nationale Supérieure de Chimie de Mulhouse, UHA, 3 rue Alfred Werner, 68093 Mulhouse Cedex, France*

^b *Groupe des Matériaux Inorganiques, Institut de Physique et Chimie des Matériaux de Strasbourg, UMR 7504 CNRS-ULP, 23 rue du Loess, 67034 Strasbourg Cedex, France*

^c *Laboratoire de Chimie de Coordination, Institut de Chimie, UMR 7177 CNRS, Université Louis Pasteur, 4 rue Blaise Pascal, 67070 Strasbourg Cedex, France*

^d *Groupe de Recherche Matériaux Hybrides Organisés Multifonctionnels, GDR 2922 CNRS, 23 rue du Loess, 67034 Strasbourg Cedex, France*

Abstract

A novel approach to incorporate transition metals into porous structures is presented, which makes use of a cobalt soap in combination with the templating agent C₁₆TMABr. An ordered mesoporous silica MCM-41 type material doped with Co is obtained after removal of the organic part by calcination. The *a* unit cell parameter of the cobalt containing mesoporous matrices is larger than that of pure MCM-41 and increases with the amount of cobalt present in the sample as well as the diameter of the pores. This is not observed when e.g. cobalt acetate is employed instead of the metal soap. The procedure presented establishes a new route for the incorporation of a transition metal into MCM-41 together with a tuning of the porous structure.

Keywords: Mesoporous material; MCM-41; Cobalt soap; Co-templating; Metal doped silica; Magnetism

1. Introduction

Since the discovery in 1992 of the M41S family of silicate mesoporous sieves with a remarkable large and uniform pore structure [1], considerable efforts have been directed towards the incorporation of transition metals inside mesoporous matrices. This can be achieved by impregnation of salts [2] or of molecular precursors [3],

grafting [4], ion exchange [5], chemical vapour deposition, etc. [6].

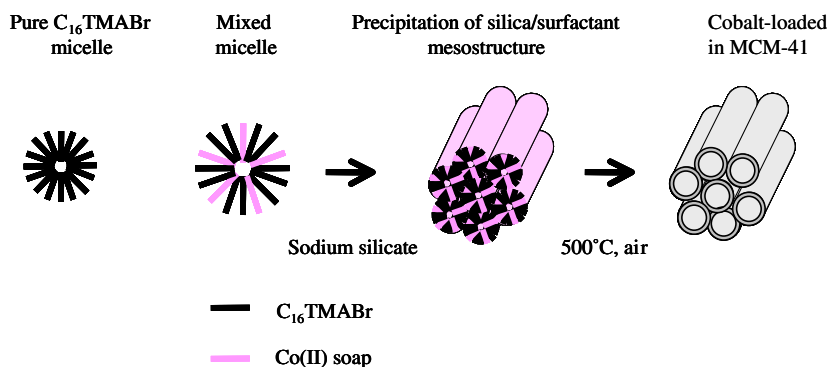
The incorporation of amphiphile molecules in the micelles of M41S-type materials is attracting increasing attention, particularly of dye molecules, which are organized inside the soap micelles [7]. A recently developed strategy consists in the use of metal-containing templates [8] or the addition of metal complexes into the precursor micelle used as template for the synthesis of the mesoporous silicate phase [9–11], leading in particular to interesting catalytic applications [12–14]. It has been shown also that lyotropic mixed-surfactant liquid-crystal templates can be used to prepare noble metal nanostructures [15,16].

Here, we describe the first use of a simple long chain metal soap to co-direct the synthesis of a metal-modified mesoporous material. It is expected with such molecules,

* Corresponding authors.

E-mail addresses: pierre.rabu@ipcms.u-strasbg.fr (P. Rabu), Jean-Louis.Paillaud@uha.fr (J.-L. Paillaud), braunst@chimie.u-strasbg.fr (P. Braunstein).

¹ Present address: CIRIMAT, UMR 5085 CNRS-UPS-INP, 118 route de Narbonne, 31062 Toulouse Cedex 04, France.



Scheme 1. Schematic representation of the proposed template mechanism involving cobalt(II) soap.

that mixed micelles can be formed between the soap and the surfactant due to strong lipophilic interactions between the long alkyl chains of each component. Indeed, recent studies have shown that it is possible to stabilize mixed micelles incorporating sodium oleate or sodium dehydrocholate with the usual surfactant cetyltrimethylammonium bromide ($C_{16}TMABr$) and that such systems can be effective MCM-41 precursors [17,18]. Moreover, the use of mixed cationic and anionic surfactants as templates was shown to be a good strategy for controlling the formation of cubic or hexagonal mesoporous materials [19,20]. On the basis of these studies, the negatively charged carboxylate moieties of the cobalt soap could be attracted by the positively charged ammonium heads of the $C_{16}TMABr$ surfactant, thus favouring the formation of mixed micelles with a parallel arrangement of the two components. As shown for other sources of cobalt, the metal ions can react with the hydroxide anions present in the alkaline media required for the formation of silica around the micelles [21]. When metal carboxylates are used, competing complexation can result. Also the combination with bromide cannot be ruled out.

The attractiveness of the cobalt soaps resides in the simplicity of their synthesis and in the ease with which the length of the alkyl chain can be adjusted to the size of the targeted micelles [22–24]. Long chain cobalt alkanates present an hexagonal columnar liquid-crystal mesophase above temperatures in the range 85–115 °C depending on the chain length, but no micellar phase is observed in water. Furthermore, we have prepared solutions of cobalt soaps in *n*-alkanes such as *n*-hexane, which provided evidence for efficient lipophilic interactions between the alkyl chains of the carboxylates and the solvent. We thus considered mixing the soap with the usual micellogen $C_{16}TMABr$ in order to induce the formation of a “mixed” micellar MCM-41-type structure where the cobalt soap would act as a co-templating agent. Preferential van der Waals interactions between long alkyl chains of each moiety are expected to stabilize the mixed structure, at least within a certain domain of Co soap concentration. For this purpose, cobalt dodecanoate $[Co\{CH_3(CH_2)_{10}COO\}_2](H_2O)_2$ was chosen for its similar chain length to that of the

$C_{16}TMABr$ molecule. The synthesis of the mesoporous material was inspired from Voegtlin et al. [25] and is illustrated in Scheme 1.

The structural and physico-chemical characteristics of the Co-MCM-41 derived from the soap were compared to those obtained with cobalt acetate in order to evaluate the intrinsic effects of the metal soaps.

2. Experimental

2.1. Characterization

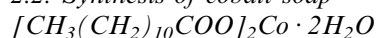
The X-ray diffraction (XRD) patterns of the samples were recorded using a PHILIPS PW 1800 diffractometer operating with Cu $K\alpha$ radiation ($\lambda = 1.5418 \text{ \AA}$).

The N_2 sorption isotherms of the materials were measured at 77 K using a Micromeritics ASAP2010 sorption analyzer. The surface area was determined according to Brunauer–Emmett–Teller (BET) method [26]. The pore size distribution was calculated using the Barrett–Joyner–Halenda (BJH) model [27]. All the samples were degassed at 423 K under vacuum before analysis.

The chemical composition of the as-synthesized samples was determined by using a MagiX Philips, X-ray fluorescence spectrometer. Elemental chemical analyses of C, H, and N were performed by the “Service Central de Microanalyses du CNRS” (Université Louis Pasteur, Strasbourg, France). Transmission electron microscopy (TEM) investigations were made using a FEI Tecnai 20F electron microscope operating at 200 kV. The samples were sonicated in ethanol and deposited on a holey copper grid. UV/visible-NIR measurements were performed with a Perkin–Elmer Lambda 19 instrument (spectra recorded by reflection with a resolution of 4 nm and a sampling rate of 250 nm/min). FT-IR studies were performed with a Digilab FTS 3000 computer driven instrument (0.5 mm thick powder samples in KBr). Magnetic studies were carried out using a Quantum Design SQUID MPMS-XL magnetometer (5 T, 2–300 K) on powder samples. The ^{29}Si solid-state NMR spectra were recorded on a Bruker MSL-300 spectrometer using a 7 mm rotor and with a magic angle spinning speed of 4.0 kHz. The acquisition parameters were $\pi/6$ for the flip

angle, and pulse duration of 1.7 μ s, 60 s for the recycle time and 577 scans. The chemical shifts are relative to tetramethylsilane (TMS). The size of the micelles was evaluated from dynamic light scattering (DLS) technics with a Malvern Instruments nano-zetasizer.

2.2. Synthesis of cobalt soap



The synthesis of the cobalt soap $[\text{CH}_3(\text{CH}_2)_{10}\text{COO}]_2\text{Co} \cdot 2\text{H}_2\text{O}$ was based on the procedure described in the literature [22,23]. Briefly:

- (1) $\text{CH}_3(\text{CH}_2)_{10}\text{COOH} + \text{KOH} \rightarrow \text{CH}_3(\text{CH}_2)_{10}\text{COOK} + \text{H}_2\text{O}$: KOH (0.1 N) in 150 ml acetone was added dropwise to an equivalent of dodecanoic acid (0.1 N) in 500 ml acetone, under reflux. A white precipitate of $\text{CH}_3(\text{CH}_2)_{10}\text{COOK}$ formed and reflux was maintained for 3 h. The solid was filtered and washed with hot acetone, and dried under vacuum.
- (2) $2\text{CH}_3(\text{CH}_2)_{10}\text{COOK} + \text{Co}(\text{CH}_3\text{COO})_2 \cdot 4\text{H}_2\text{O} \rightarrow [\text{Co}\{\text{CH}_3(\text{CH}_2)_{10}\text{COO}\}_2] \cdot 2\text{H}_2\text{O} + 2\text{H}_2\text{O} + 2\text{CH}_3\text{COOK}$: A solution containing 4.00 g of $\text{CH}_3(\text{CH}_2)_{10}\text{COOK}$ in 150 ml water and 150 ml ethanol under argon was added dropwise, under vigorous stirring, to an aqueous solution of 2.09 g of $[\text{Co}(\text{CH}_3\text{COO})_2] \cdot 4\text{H}_2\text{O}$. After the mixture was stirred for 3 h, the pink precipitate formed was filtered, washed with water and ethanol, and dried under vacuum.

2.3. Synthesis of Co-MCM-41

Cetyltrimethylammonium bromide ($\text{C}_{16}\text{TMABr}$) was used as a templating agent (Fluka). Sodium silicate was used as a silica source (27 wt% silica, Riedel de Haën). The cobalt soap $[\text{CH}_3(\text{CH}_2)_{10}\text{COO}]_2\text{Co} \cdot 2\text{H}_2\text{O}$ and cobalt acetate $\text{Co}(\text{CH}_3\text{COO})_2 \cdot 4\text{H}_2\text{O}$ (Fluka) were used as Co precursors. Hydrochloric acid (Riedel de Haën) was used to adjust the pH of the solution.

The molar composition is $1.0\text{SiO}_2:0.4\text{Na}_2\text{O}:0.2\text{C}_{16}\text{TMABr}:135\text{H}_2\text{O}:0.022\text{HCl}:x\text{Co}$ with $x = 0.005\text{--}0.040$ for the soap and $x = 0.010\text{--}0.040$ for the acetate. $\text{C}_{16}\text{TMABr}$ (1.724 g) was dissolved in 35 g of water with stirring at about 308 K to obtain a clear micellar solution. Then, the cobalt compound was added giving a pale pink solution. Separately, at room temperature, 5.25 g of sodium silicate was dissolved in a sodium hydroxide solution (0.21 g of NaOH in 5.45 g of water) with stirring for 2 min. Then, the silicate solution was added to the micellar solution which turned to purple-blue. Precipitation was observed immediately. After stirring for 10 min, about 16 ml of HCl 1 M was introduced dropwise to reach a pH of 8.5. After stirring for 1 h, the resulting gel was transferred into a polypropylene bottle and kept in an oven at 373 K for 24 h. The resulting solid was recovered by filtration, washed with distilled water and dried under ambient condi-

Table 1

X-ray fluorescence spectrometry analysis of the relative Co content for the Co-MCM-41 compounds synthesized with cobalt soaps (b–e) or cobalt acetate (f–h)

Sample	Cobalt precursor	Molar ratio		
		Co precursor $\text{C}_{16}\text{TMABr}$	Si/Co in the initial gel	Final Si/Co in the sample
a	–	0	∞	∞
b	Soap	0.025	197	226
c	Soap	0.05	99	111
d	Soap	0.1	49	53
e	Soap	0.2	24	27
f	Acetate	0.05	100	111
g	Acetate	0.1	50	55
h	Acetate	0.2	25	26

tions. Finally, the materials were calcined in a furnace at 813 K for 4 h in air, to remove the residual organics.

A pure siliceous MCM-41 was also prepared following the procedure described above for Co-MCM-41, without incorporating the cobalt source into the synthesis solution and before it was kept in an oven at 363 K, the gel was stirred for 2 h.

Samples with different cobalt contents are referred to as a for pure silica MCM-41, b, c, d, and e, for those based on the cobalt soap and f, g and h for those based on cobalt acetate (Table 1).

3. Results and discussion

3.1. Synthesis and chemical analysis

The cobalt soap $[\text{Co}\{\text{CH}_3(\text{CH}_2)_{10}\text{COO}\}_2](\text{H}_2\text{O})_2$ was synthesized according to the procedure described in the literature and used as a co-template in the synthesis of the mesoporous solid (see Section 2) [22,23]. The procedure used for the synthesis of Co-MCM-41 in presence of cobalt soap is derived from that for pure MCM-41, described by Voegtlin et al. [25]. They have shown that the adjustment of the pH at 8.5 by hydrochloric acid makes it possible to obtain a well organized mesostructure MCM-41. The procedure consists in the synthesis of MCM-41 by addition of the cobalt soap to the micellar solution of $\text{C}_{16}\text{TMABr}$. A mixture of $\text{C}_{16}\text{TMABr}$ and cobalt soap was used of which the amount of cobalt was varied so that the Si/Co molar ratio was in the range 24–198 while keeping the $\text{C}_{16}\text{TMABr}/\text{Si}$ ratio constant. The lower limit of the Si/Co ratio (24) corresponds to the maximum solubility of the cobalt soap in the present MCM-41 synthesis medium. It is worth noticing here that the occurrence of a precipitate for such quite small amount of cobalt indicates that the situation is different from a simple dissolution of the soap in the hydrophobic region of the $\text{C}_{16}\text{TMA}^+$ moieties. Actually, the latter would imply weak ionic interaction between the carboxylate and ammonium heads, which is unlikely (see above).

The relative mass percents of cobalt and other elements (excepted H) were determined by X-ray fluorescence

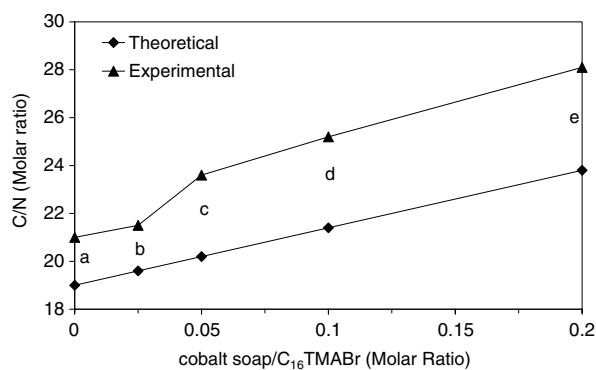


Fig. 1. Comparison of C/N molar ratios between the expected values and chemical analysis of as-synthesized samples a, b, c, d, e vs the cobalt soap/ C_{16} TMABr molar ratio of the initial gels.

spectrometry on the as-synthesized materials (Tables 1 and SM1), and we consider that the Co content does not change after calcination. The results show for all the samples that the amount of cobalt in the MCM-41 is almost 100% of that introduced in the starting precursor. It shows that in the synthesis condition used here all the cobalt has precipitated as $Co(OH)_2$ that interacted with the silica precursors [21]. To ascertain that the Co soap is present as a whole (not only Co^{2+} ions) in the as-synthesized materials, the variation of the C/N ratio as a function of the amount of Co introduced was investigated on the basis of the chemical C, H, N analyses (Table SM2). The result is presented as a graph in Fig. 1 and is compared to the theoretical ratio expected from the relative Co soap vs C_{16} TMABr amounts in the initial mixture (Table SM2). It appears that the C/N ratio increases with the Co content and is always slightly higher than the theoretical one, which indicates a real incorporation of the soap.

In order to demonstrate further the interest of using a cobalt soap and to evaluate its co-templating effect compared to the simple addition of other metal salts, Co-MCM-41 materials were synthesized by using cobalt acetate, $Co(CH_3COO)_2 \cdot 4H_2O$, which is more appropriate for comparison with the soap than other cobalt sources used in the literature, owing to the presence of the carboxylate groups. Various amounts of cobalt acetate were introduced during the synthesis of the MCM-41 similarly to the cobalt soap in the former series, i.e., just after having prepared the micellar solution with the C_{16} TMABr surfactant (see Section 2.3).

The amount of cobalt effectively incorporated in the samples was measured by X-ray fluorescence analysis and the results given in Table SM3 and summarized in Table 1 show a good agreement between the initial amounts in the precursor and those in the final Co-MCM-41.

3.2. Powder X-ray analysis

The powder XRD patterns (Fig. 2) of the as-synthesized samples obtained with the cobalt soap show four peaks for

the samples a–d and only three for the sample e, with the largest quantity of cobalt, which appears less well organized than the others. In general, the diffractograms are less resolved when the amount of cobalt soap added increases in the preparation. The peaks are characteristic of MCM-41 mesostructures with a hexagonal cell. As shown in Table 2, the calculated unit cell parameter $a_0 = 2d_{10}/\sqrt{3}$ increases with the amount of cobalt in the samples, which indicates either an increase of the pore size or larger walls. This point will be settled below on the basis of the nitrogen adsorption measurements.

The powder XRD patterns of the samples calcined at 813 K in air (see Section 2.3) are displayed in Fig. 2. Compared to the as-synthesized materials, the resolution of the powder X-ray diffractogram decreases again when the cobalt soap amount increases. No peak is observed in the $10\text{--}70^\circ$ 2θ range that could have indicated the formation of cobalt oxide, but this could be due to a too low metal content (Table SM1). Only the peaks characteristic of the MCM-41 are present, at low angles, which were indexed according to a hexagonal structure and the calculated cell parameters are listed in Table 2. Similarly to as-synthesized samples, the unit cell parameter value increases with the amount of cobalt in the samples. The cell parameter cannot be calculated for the sample with the largest cobalt content (sample e), for which only a broad peak at low angle is observed, denoting a poor organization of the mesostructure.

Similarly, the powder XRD patterns of the as-synthesized and calcined samples obtained from cobalt(II) acetate show four peaks, corresponding to MCM-41 (Fig. 3). No significant peak was detected above $2\theta = 10^\circ$.

The calculated unit cell parameter of each sample before and after calcination is given in Table 2. A slight increase of this value compared to the sample of MCM-41 without cobalt is noted, but in contrast to the previous series, no significant change occurs as a function of the cobalt amount (Fig. 4). This result is in agreement with those obtained with the other cobalt complexes cited above [10–14]. Moreover, all the samples obtained with cobalt(II) acetate exhibit similar X-ray patterns, showing that, contrarily to the soap, its presence has little influence on the crystallographic order of the mesoporous solids.

When the amount of cobalt increases, the samples synthesized in the presence of cobalt acetate are more organized than those synthesized with the cobalt soap. This difference can be explained by the fact that the metal soap is incorporated into the C_{16} TMABr micelles due to ionic and lipophilic interactions but, at high concentrations, the soap, that does not form micelles alone, weakens the cohesion of the micelle, which is essentially maintained by the C_{16} TMABr surfactant. In addition, it has been shown that a combination of anionic surfactants with the cationic $C_{16}TMA^+$ reduces the positive charge of the micelle surface thus weakening the rigidity of the micelle [19]. Charge effects related to the addition of increasing amounts of cobalt salts were also suggested for explaining

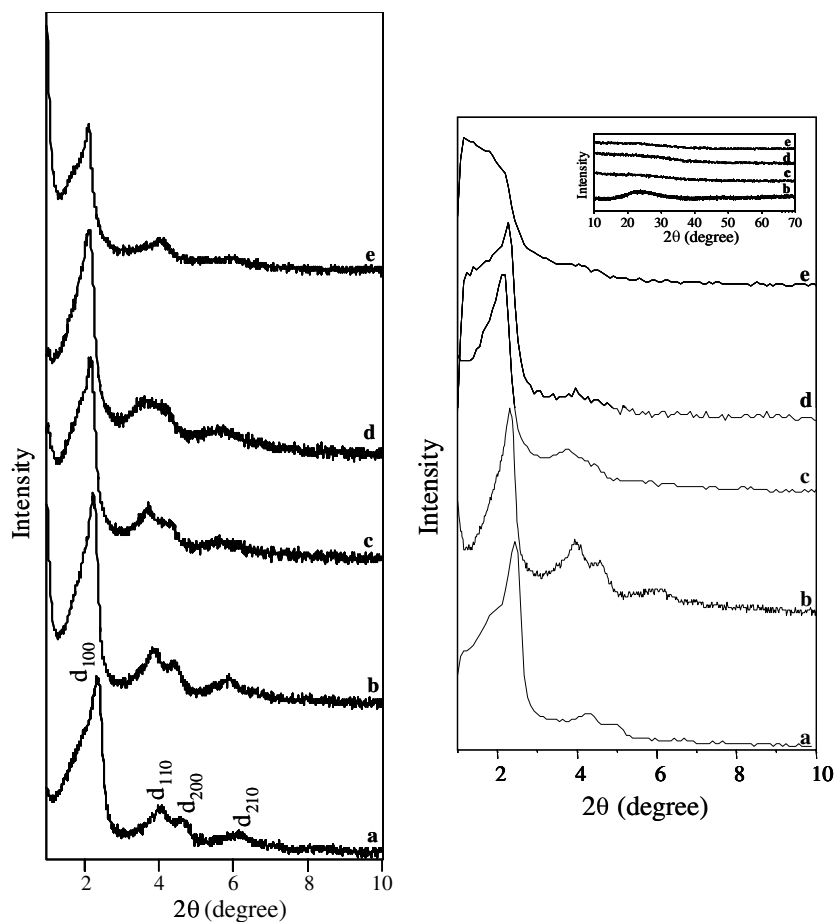


Fig. 2. X-ray diffraction powder patterns of as-synthesized samples (left) and calcined samples (right) with different amounts of cobalt soap a: MCM-41; b, c, d, e: Co-MCM-41 (b: $x = 0.005$; c: $x = 0.01$; d: $x = 0.02$; e: $x = 0.04$).

Table 2
 d_{10} Spacings and unit cell parameters (a_0) of the pure siliceous MCM-41 (a) and Co-MCM-41 samples synthesized with cobalt soap (b–e) or cobalt acetate (f, g) before and after calcination

Sample	Cobalt precursor	Molar ratio $\frac{\text{Co precursor}}{\text{C}_{16}\text{TMABr}}$ (initial gel)	Before calcination		After calcination	
			d_{10} (nm)	a_0 (nm)	d_{10} (nm)	a_0 (nm)
a	–	0	3.64	4.2	3.61	4.2
b	Soap	0.025	3.86	4.4	3.78	4.3
c	Soap	0.05	3.97	4.5	3.87	4.4
d	Soap	0.1	4.12	4.7	4.07	4.7
e	Soap	0.2	4.17	4.8	–	–
f	Acetate	0.05	3.79	4.4	3.72	4.3
g	Acetate	0.1	3.78	4.4	3.64	4.2
h	Acetate	0.2	3.77	4.4	3.68	4.3

a structural change of mesoporous silica, from cubic to hexagonal for instance [21].

3.3. Transmission electron microscopy

The as-synthesized mesostructure was directly observed by transmission electron microscopy (TEM) on several

samples (Fig. 5). Observation of as-synthesized sample b indicates large coherence domains with comparable hexagonal periodicities and no amorphous zone. In turn, the cobalt-rich sample c appears less organized, with smaller coherence length, and contains amorphous zones. In the latter case, two different pore stacking periodicities were detected ($d_{100} = 4.4$ nm and 3.7 nm) in different areas. The presence of different domains corresponding to different cell parameter values is consistent with the X-ray diffraction patterns, the quality of which decreases with higher cobalt contents (Fig. 2). Similar TEM images were observed after calcination which does not modify the mesostructures.

3.4. Nitrogen adsorption measurements

Nitrogen adsorption was measured on the different calcined samples in order to characterize their porosity. All isotherms of adsorption are of the type IV according to the IUPAC classification (Fig. 6) and are typical of mesoporous materials [28]. The isotherms of the Co-MCM-41 samples are comparable with that of pure MCM-41. All the values deduced from the adsorption isotherms are summarized in Table 3.

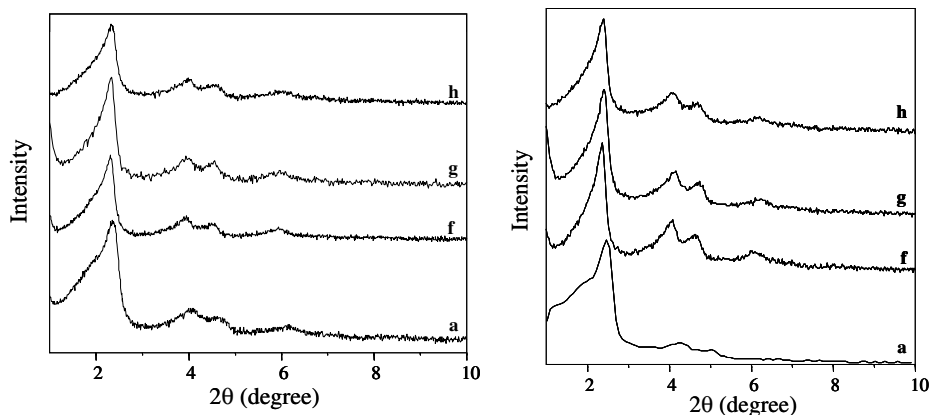


Fig. 3. X-ray diffraction before (left) and after (right) calcination, a: MCM-41; f, g, h: Co-MCM-41 (a: $x = 0.0$, f: $x = 0.010$; g: $x = 0.020$; h: $x = 0.040$).

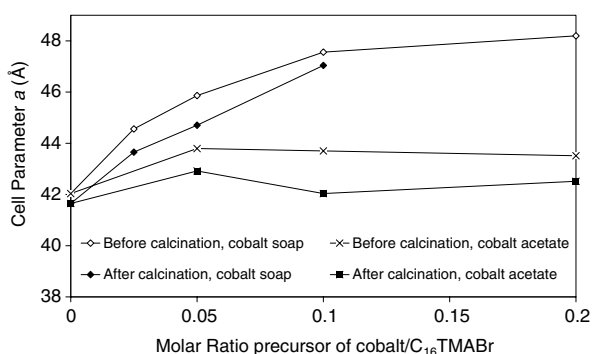


Fig. 4. Comparison of the unit cell parameter a before and after calcination according to the source of cobalt used.

The isotherms show the presence of two types of mesopores. For $P/P_0 < 0.4$, they are small mesopores. The absence of a hysteresis in the desorption curve below this point is characteristic of the presence of small mesopores with a narrow distribution of the pore size and is typical of MCM-41 materials. The corresponding mesoporous volume for $P/P_0 < 0.4$ increases and the BET surface area decreases with the cobalt soap content as shown by the shift of the step towards higher pressures observed in the isotherms. This is in accordance with the results of Kong et al. in the case of MCM-48-type materials prepared in presence of $C_{16}TMABr/Na$ -Laurate mixed micelles [19].

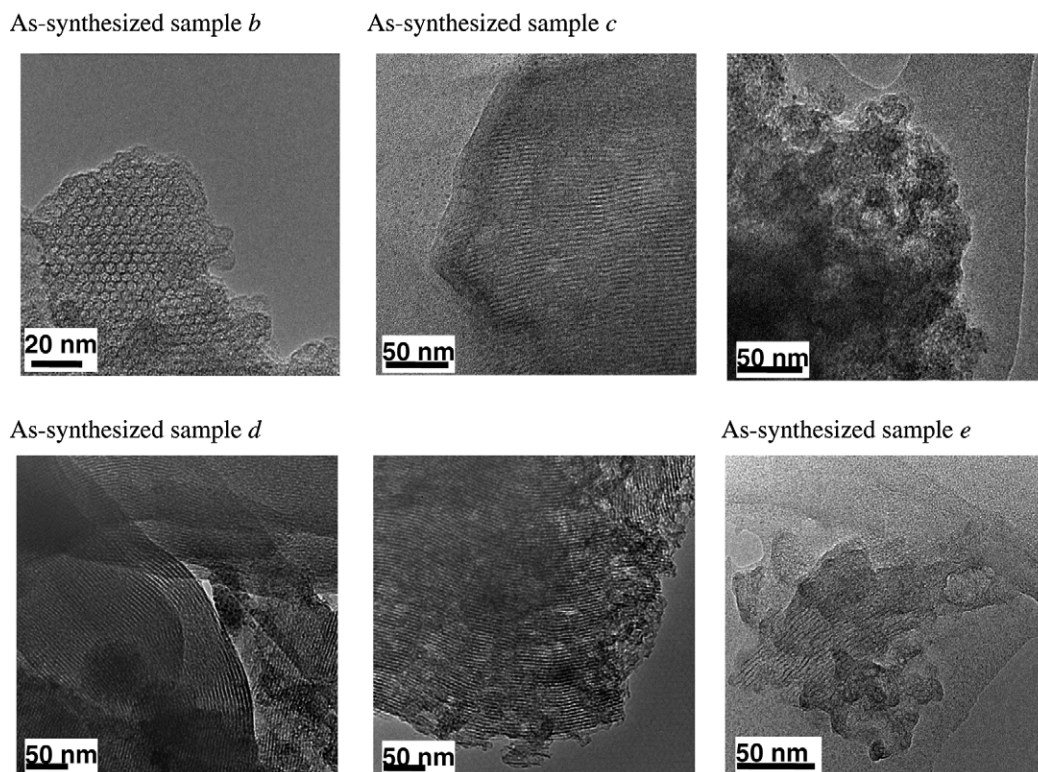


Fig. 5. TEM images of samples *b*, *c*, *d* and *e* before calcination.

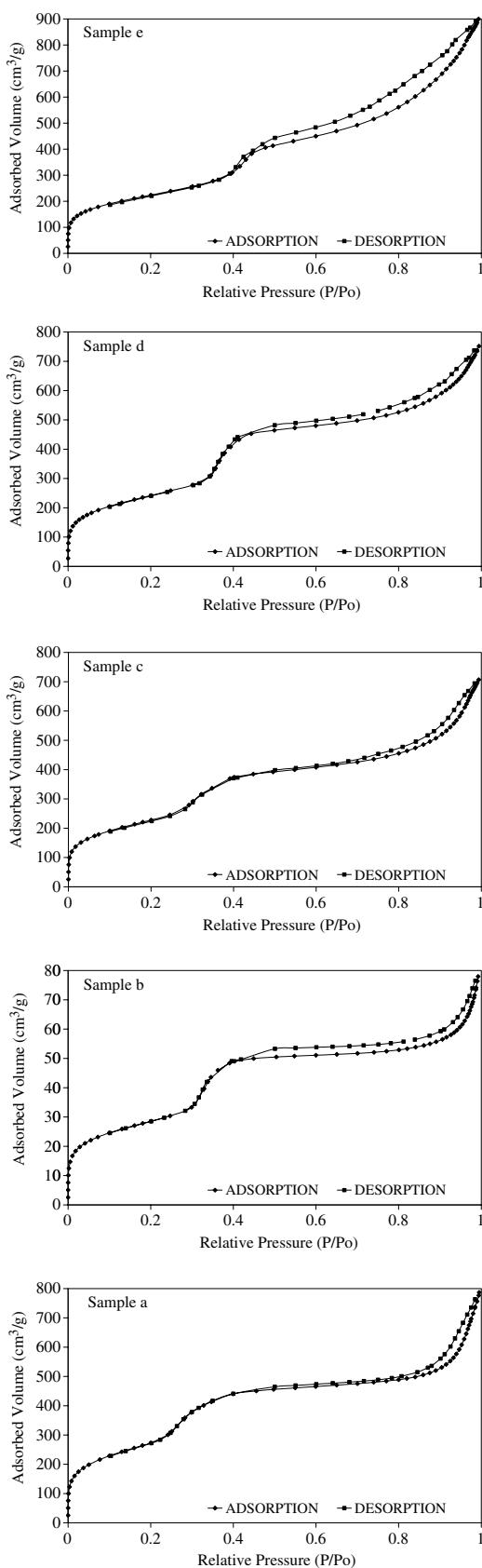


Fig. 6. N_2 adsorption-desorption isotherms of calcined samples a, b, c, d and e.

The upward trend of the curves for higher P/P_0 (for $P/P_0 > 0.4$) values is related to inter granular mesopores of larger size, probably macropores. The presence of a narrow hysteresis for all samples is assigned to mesopores with narrow apertures.

Moreover, this hysteresis becomes more important when the amount of cobalt increases in the samples. This last point is the most pronounced for the Co rich sample e. This phenomenon may be related to an increase in the dispersion of the pore size distribution and a partial loss of the mesopore organization. This is in agreement with the PXRD results.

For the cobalt soap derived samples, a “*t*-plot” analysis indicates the presence of a very small amount of micropores (less than 1% of the total volume).

Thus, the size of the pores increases with the cobalt content but the thickness of the walls remains almost unchanged in the presence of the cobalt soap. This is a first indication that the size of the micelles is influenced by the incorporation of the metal soap. Such variation of size is related to a surface curvature modification, which might be consistent with the presence of metal alkylcarboxylate incorporated within the micelles. This is a very different situation from that encountered when cobalt(II) nitrate, sulphate, chloride or atrane complexes are used [10–14], where an increase of the wall thickness was observed whereas the pore size was almost unaffected by the presence of metal salt in the micellar precursor. The fact that the thickness of the walls in the present Co-MCM-41 materials remains unchanged upon addition of cobalt soap is strongly in favour of the Co(II) ions being located at the surface of the micelle, and thus inside the pores in the final product.

The samples g and h obtained with cobalt acetate were analyzed similarly by nitrogen adsorption. The isotherms (adsorption-desorption) are of type IV – H1 according to the IUPAC classification. The samples do not show microporosity. Compared to pure MCM-41, the pore size is larger but does not vary with the amount of Co(II) acetate. This may suggest that the cobalt acetate is merely at the external surface of the C_{16} TMABr micelles, contributing to larger pore size but without affecting the size of the micelle itself. Compared now to related samples prepared with the cobalt soap, the size of the pores and the thickness of the walls are smaller (Table 3), which indicates that cobalt acetate was not incorporated in the same way as the cobalt soap. The decrease of the BET surface area with increasing quantity of cobalt is slightly smaller compared to that observed with the cobalt soap ($1051\text{--}992\text{ m}^2/\text{g}$ compared with $870\text{--}804\text{ m}^2/\text{g}$ for the same quantities of cobalt).

3.5. Sizes of the micelles

In order to compare directly the effect of the two cobalt sources, the size of the micelles obtained when mixing them with water but without silica source was tentatively investigated by using a nanosizer (see Section 2.1). This

Table 3

Porous characteristics of the pure siliceous MCM-41 (a) and Co-MCM-41 samples obtained with cobalt soap (b–e) or cobalt acetate (f, g)

Sample	Molar ratio $\frac{\text{Co precursor}}{\text{C}_{16}\text{TMABr}}$ (initial gel)	Cobalt precursor	$S_{\text{BET}}^{\text{a}}$ (m^2/g)	V_{t}^{b} (cm^3/g)	$V_{\text{micro}}^{\text{c}}$ (cm^3/g)	$V_{\text{meso}}^{\text{d}}$ (cm^3/g)	\varnothing pores ^e (nm)	Wall thickness ^f (nm)
a	0	–	1029	0.75	–	0.75	2.58	1.59
b	0.025	Soap	1024	0.80	0.05	0.75	2.85	1.51
c	0.05	Soap	832	0.75	–	–	2.96	1.51
d	0.1	Soap	870	0.81	0.01	0.80	3.10	1.60
e	0.2	Soap	804	0.93	0.01	0.92	3.62	–
g	0.1	Acetate	1051	0.84	–	0.84	2.80	1.4
h	0.2	Acetate	992	0.86	–	0.86	2.86	1.43

^a BET surface area.

^b V_{t} , total porous volume.

^c V_{micro} , microporous volume calculated from the t -plot method.

^d V_{meso} , mesoporous volume determined from the relation $V_{\text{meso}} = V_{\text{t}} - V_{\text{micro}}$.

^e Determined from the desorption branch by BJH method.

^f Thickness of the walls calculated from the relation: a – pore diameter.

technique, usually used for the determination of the size of small particles in suspension, gives the effective size of the objects, here the micelles, diffusing the light of a laser beam. The results of the measurements carried out on cobalt soap/water and cobalt acetate/water mixtures with identical ratios to those used for samples a, b, c on the one hand and f, g on the other hand are presented in Fig. 7. It suggests that the effective size of the micelles increases rapidly, up to 6.5 nm for 5% of Co, upon addition of soap and

much more than with acetate for which the effective size does not exceed 3.2 nm for 10% of Co. In the case of the cobalt soap, an additional peak around 2 nm is also observed for the 5% Co sample, which can be interpreted as due to a multimodal size distribution and is consistent with the (meso)-structural heterogeneity observed for the sample with large Co soap amount. All these results are in agreement with those observed by Kong et al. in the mixed CTMABr/Na-Laurate system [19]. Indeed, the introduction of our cobalt soap, like the Na-Laurate into the cationic surfactant, increases the flexibility of the micelles.

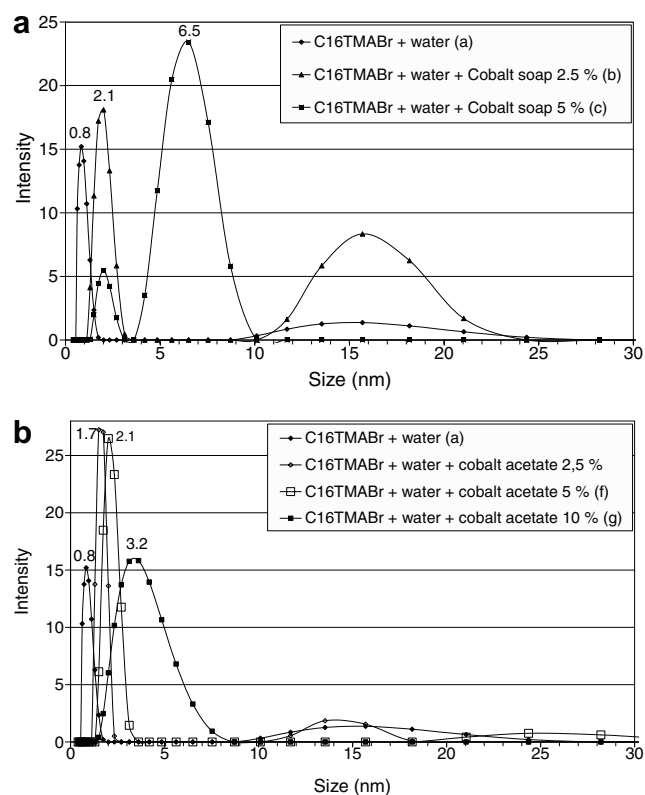


Fig. 7. Size of micelles prepared from $\text{C}_{16}\text{TMABr}$, water and (a) cobalt soap with identical ratios to those used for compounds a, b, c, and (b) cobalt acetate with identical ratios to those used for compounds a, f, g.

3.6. ^{29}Si MAS NMR spectroscopy

An analysis by ^{29}Si MAS NMR of as-synthesized and calcined samples synthesized with soap was performed to study the influence of the presence of cobalt on the proportion of the different Q^n units ($Q^n = (\text{SiO})_n\text{Si}(\text{OH})_{4-n}$).

Representative ^{29}Si MAS NMR spectra of the calcined samples are given in Fig. 8 (other spectra are given in the Supplementary Material, Figs. SM1 and SM2). On all spectra, only the two silicon types Q^3 and Q^4 are observed at -100 and -109 ppm, respectively. The relative amount of silicate species were calculated from the NMR spectra simulations, the proportions of which are given in Table 4.

The spectra of as-synthesized samples (Fig. SM1) show that the contribution of the Q^n sites (Q^3 , Q^4) is similar throughout the whole sample series, including Co-MCM-41 and pure MCM-41 derivatives, which is again consistent with the fact that the Co(II) ions do not influence much the internal structure of the silica walls.

The ^{29}Si MAS NMR spectra of calcined samples a and e are compared in Fig. 8. Both spectra were recorded under the same conditions on the same amount of materials and with the same number of scans. Signals characteristic of Q^3 and Q^4 species are present in samples a and e. However, their intensity decreases in the case of the Co-containing

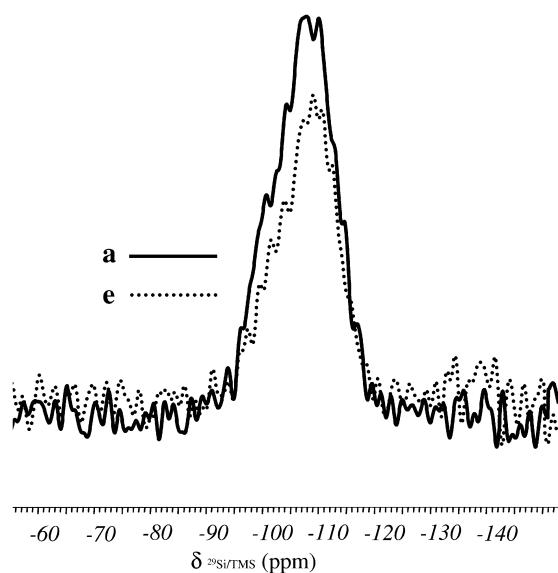


Fig. 8. ^{29}Si MAS NMR spectra of calcined samples: pure MCM-41 (sample a) and Co-MCM-41 (sample e).

MCM-41 sample e. This is due to the proximity of paramagnetic, cobalt(II) centres near the silicon nuclei. The presence of cobalt affects the species Q^3 and Q^4 in the same way. El Haskouri et al. [12] have observed similar effects and Casu et al. [29] have obtained similar results for the interactions of iron with silica matrices.

3.7. Infrared spectroscopy

The local structure of these cobalt containing mesostructures was investigated by Fourier transformed infrared (FTIR) spectroscopy carried out on the different Co-MCM-41 samples and compared to that of the pure MCM-41 without Co(II) soap (see Fig. SM3 in Supplementary Material). The spectrum of pure MCM-41 exhibits characteristic absorption bands for $\nu(\text{OH})$ (broad at 3400 cm^{-1}), $\nu(\text{CH})$ (strong at 2920 and 2850 cm^{-1}) and silicate (strong broad between 1250 and 1000 cm^{-1}), in agreement with the presence of alkyl ammonium surfactant in the silica network. When the cobalt soap is introduced, additional bands at 1570 and 1480 cm^{-1} are observed, which are characteristic of antisymmetrical and symmetrical $\nu(\text{CO})$ vibrations. This definitely supports the presence of the alkylcarboxylate introduced with the soap into the micellar precursor. Moreover, the difference between these two bands, $\Delta\nu = 90\text{ cm}^{-1}$, is consistent with coordinated

Table 4
Relative amounts of the Si sites determined by ^{29}Si MAS NMR in calcined samples a and e

		Q^3	Q^4
a Calcined	δ (ppm)	-101	-109
	%	15	85
e Calcined	δ (ppm)	-101	-109
	%	16	84

carboxylates, although they are bonded in a different way than in the starting Co soap that exhibits a mixed bidentate/chelate mode with $\Delta\nu = 125\text{ cm}^{-1}$ [24]. After calcination, in the FTIR spectrum of sample e for instance, the $\nu(\text{CH})$ and $\nu(\text{CO})$ bands vanish owing to the burning of the carbon skeleton and only characteristic bands of hydroxyl groups and silica are observed.

3.8. UV spectroscopy

The question remains of the nature of the cobalt in the materials. In order to investigate the oxidation state of the cobalt ions in the mesoporous solids, the powder samples were analyzed by UV reflectance spectroscopy. The spectra in Fig. 9 show characteristic absorption bands for Co^{2+} in tetrahedral and octahedral coordination geometries [30,31] in agreement with the purple-blue color of the as-synthesized products. It is noteworthy that the molar absorption coefficient for tetrahedral species is much higher than for the octahedral ones, usually masking the latter contribution in the electronic spectra when both are present. Thus, we may assume that in the present compounds, the tetrahedrally coordinated ions correspond to the minor species. Such tetrahedral coordination is not observed in the starting hydrated cobalt(II) soaps, thus mitigating the possibility of $\text{C}_{16}\text{TMABr}$ would merely solubilize the soap, unless the carboxylate would experience a strong structural rearrangement. This is in agreement with the IR results discussed above. The occurrence of octahedral sites suggests a slightly different situation to that mentioned by Vrålstad et al. [21] who identified only isolated tetra- or pentacoordinated cobalt species from EXAFS analysis. This result could be explained by different synthesis conditions. The calcined sample are more blue in accordance with a tetrahedral coordination for the cobalt. However, the UV/visible spectrum of calcined sample e (Fig. 9) still shows the presence of octahedrally coordinated Co species.

After calcination, although the formation of particles inside the pores can be expected, they are apparently not

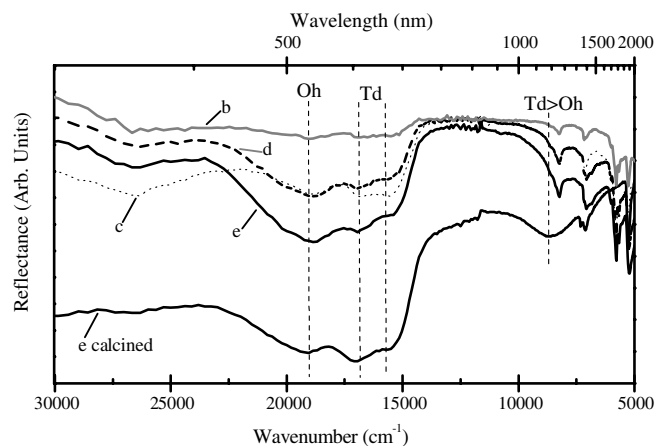


Fig. 9. UV/visible spectra of the as-synthesized samples Co-MCM-41 b-e and the calcined sample e.

in sufficient amount and/or too small to be identified by powder X-ray diffraction. Actually, the mass percent of Co in the samples is very small (less than 3.5%) and particles situated inside the silica channels, the diameter of which is about 3 nm, would be necessarily smaller. Even TEM observation is illusive due to poor contrast between Co and organized mesoporous silica. Cobalt nanoparticles were observed by TEM only after heating the samples at high temperature (700–900 °C) under hydrogen. In that case indeed, particles with diameters larger than 25 nm are observed (Fig. SM4) and the initial mesostructure is strongly deteriorated.

3.9. Magnetic measurements

These results are consistent with the magnetic data obtained for the as-synthesized samples Co-MCM-41 b–e which are presented in Fig. 10. The temperature dependence of the magnetic susceptibilities scaled to the experimental Co amount are very similar for all the samples and the Curie constant $C = 3.13, 2.94, 3.23$ and $2.94 \text{ K emu mol}^{-1}$ was deduced for samples b, c, d and e, respectively, by fitting the high temperature data to the Curie–Weiss law. These values are in the expected range for octahedral Co^{2+} ions [32,33], confirming that the cobalt in the as-synthesized samples is divalent, which is consistent with the UV spectroscopy data. More surprisingly, the low temperature measurements on all compounds indicate a strong increase of the χT product when lowering the temperature, pointing to a ferromagnetic-like behavior, confirmed by the hysteresis loop observed in the magnetization vs field curve recorded at 1.8 K. This indicates, in the as-synthesized samples, the formation of extended Co(II) magnetic networks. This could correspond to the formation of cobalt silicate clusters like olivine Co_2SiO_4 which is known to behave as a frustrated antiferromagnet. It may exhibit ferromagnetism when imperfectly crystalized but contains only metal centres in octahedral sites [34,35]. A similar ferromagnetic-like behavior was also reported for Co_2O_3 particles in silica matrix [35].

All the present results support the assumption that the lipophilic chains of the cobalt soap are in the micelle struc-

ture, widening the size of the pores as a function of the Co(II) soap amount, and emphasize the specific role played by the soap compared to the simple carboxylate.

4. Conclusion

The results reported in this paper establish a new way of incorporating transition metals into porous structures, using metal soaps to generate “mixed” micelles as co-templating agents. After calcination of the mesoporous material prepared in the presence of cobalt soap, porous Co-doped silica was obtained. Although the cobalt soap does not exhibit itself a micellar phase in water, the presence of $\text{C}_{16}\text{TMABr}$ is sufficient to direct the formation of the porous structure, and the amphiphilic nature of the metallic soap ensures that the metal atoms will be involved in the micelle structure, and merely located at the surface of, or inside the pores. New cobalt-modified mesoporous materials have thus been synthesized whose specific surface area and metal content are interesting for potential application in catalysis, for instance [36]. Further investigations are currently under way in order to clarify the location of the cobalt atoms. For instance, the study of adsorption of pyridine could provide an insight into the acid sites of the pore surface [37]. The preparation of extractive replica samples for transmission electron microscopy (TEM) is envisaged for viewing small particles in the calcined Co-MCM-41 samples [38].

Acknowledgements

We are grateful to the Région Alsace (Doctoral grant to S.G.-V. and F.T.-S.) and the Centre National de la Recherche Scientifique and to the Ministère de la Recherche for support.

Appendix A. Supplementary data

Supplementary data associated with this article can be found, in the online version, at [doi:10.1016/j.micro-meso.2007.01.056](https://doi.org/10.1016/j.micro-meso.2007.01.056).

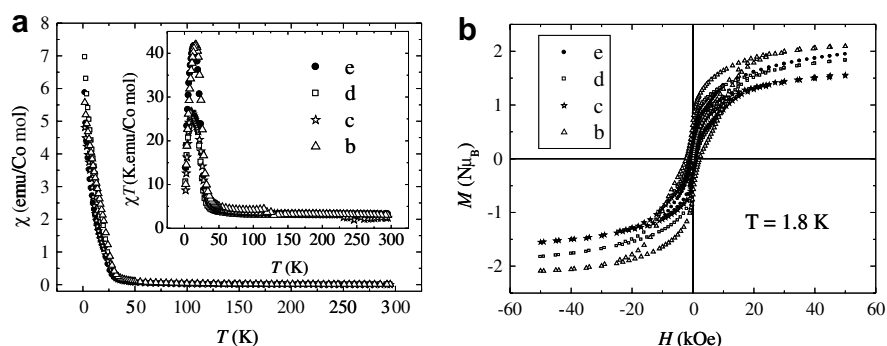


Fig. 10. Thermal variation of the magnetic susceptibility (a) and magnetization vs field cycles at 1.8 K (b) for the as-synthesized samples Co-MCM-41 b–e.

References

- [1] C.T. Kresge, M.E. Leonowicz, W.J. Roth, J.C. Vartuli, J.S. Beck, *Nature* 359 (1992) 710.
- [2] M. Sasaki, M. Osada, N. Higashimoto, T. Yamamoto, A. Fukuoka, M. Ichikawa, *J. Mol. Catal. A: Chem.* 141 (1999) 223;
M.A. Aramendia, V. Borau, C. Jiménez, J.M. Marinas, F.J. Romero, *Chem. Commun.* (1999) 873;
Y. Wang, M. Noguchi, Y. Takahashi, Y. Ohtsuka, *Catal. Today* 68 (2001) 3;
Y. Ohtsuka, T. Arai, S. Takasaki, N. Tsubouchi, *Energy Fuels* 17 (2003) 804.
- [3] Y. Guari, C. Thieuleux, A. Mehdi, C. Reyé, R.J.P. Corriu, S. Gomez-Gallardo, K. Philippot, B. Chaudret, R. Dutartre, *Chem. Commun.* (2001) 1374;
F. Schweyer, P. Braunstein, C. Estournès, J. Guille, H. Kessler, J.-L. Paillaud, J. Rosé, *Chem. Commun.* (2000) 1271;
D.S. Shepard, T. Maschmeyer, G. Sankar, J.M. Thomas, D. Ozkaya, B.F.G. Johnson, R. Raja, R.D. Oldroyd, R.G. Bell, *Chem. Eur. J.* 4 (1998) 1214.
- [4] P. Braunstein, H.-P. Kormann, W. Meyer-Zaika, R. Pugin, G. Schmid, *Chem. Eur. J.* 6 (2000) 4637;
R. Anwander, H.W. Görlitzer, G. Gerstberger, C. Palm, O. Runte, M. Spiegler, *J. Chem. Soc. Dalton Trans.* (1999) 3611.
- [5] Z. Zhang, S. Dai, X. Fan, D.A. Blom, S.J. Pennycook, Y. Wei, *J. Phys. Chem. B* 105 (2001) 6755;
Y. Zhang, Q. Zhang, T. Shishido, K. Takehira, *J. Catal.* 209 (2002) 186.
- [6] E. Lindner, T. Schneller, F. Auer, H.A. Mayer, *Angew. Chem. Int. Ed.* 38 (1999) 2154;
J.Y. Ying, C.P. Mehnert, M.S. Wong, *Angew. Chem. Int. Ed.* 38 (1999) 56;
N. Hüsing, U. Schubert, *Angew. Chem. Int. Ed.* 37 (1998) 22.
- [7] I. Honma, H.S. Zhou, *Adv. Mater.* 10 (1998) 1532;
H.S. Zhou, H. Sasabe, I. Honma, *J. Mater. Chem.* 8 (1998) 515;
F. Marlow, M.D. McGehee, D. Zhao, B.F. Chmelka, G.D. Stucky, *Adv. Mater.* 11 (1999) 632;
J. Oh, H. Imai, H. Hirashima, *Chem. Mater.* 10 (1998) 1582;
M. Ohtaki, K. Inata, K. Eguchi, *Chem. Mater.* 10 (1998) 2582.
- [8] H.B. Jervis, M.E. Raimondi, R. Raja, T. Maschmeyer, J.M. Seddon, D.W. Bruce, *Chem. Commun.* (1999) 2031.
- [9] Z.-Y. Yuan, H.-T. Ma, Q. Luo, W. Zhou, *Mater. Chem. Phys.* 77 (2003) 299.
- [10] J. El-Haskouri, S. Cabrera, C. Guillem, J. Latorre, A. Beltrán, M.D. Marcos, C.J. Gómez-García, D. Beltrán, P. Amorós, *Eur. J. Inorg. Chem.* (2004) 1799.
- [11] S. Lim, D. Ciuparu, C. Pak, F. Dobek, Y. Chen, D. Harding, L. Pfefferle, G. Haller, *J. Phys. Chem. B* 107 (2003) 11048;
P. Xue, G. Lu, Y. Guo, Y. Wang, Y. Guo, *J. Mol. Catal. B* 30 (2004) 75.
- [12] J. El-Haskouri, S. Cabrera, C.J. Gómez-García, C. Guillem, J. Latorre, A. Beltrán, D. Beltrán, M.D. Marcos, P. Amorós, *Chem. Mater.* 16 (2004) 2805.
- [13] V. Cortés Corberán, M.J. Jia, J. El-Haskouri, R.X. Valenzuela, D. Beltrán-Porter, P. Amorós, *Catal. Today* 91–92 (2004) 127.
- [14] Á. Szegedi, Z. Kónya, D. Méhn, E. Solymár, G. Pál-Borbély, Z.E. Horváth, L.P. Biró, I. Kiricsi, *Appl. Catal. A: Gen.* 272 (2004) 257.
- [15] T. Kijima, T. Yoshimura, M. Uota, T. Ikeda, D. Fujikawa, S. Mouri, S. Uoyama, *Angew. Chem. Int. Ed.* 43 (2004) 228.
- [16] N.C. King, R.A. Blackey, W. Zhou, D. Bruce, *Chem. Commun.* (2006) 3411.
- [17] N. El Kadi, F. Martins, D. Clause, P.C. Schulz, *Colloid Polym. Sci.* 281 (2003) 353.
- [18] P. Messina, M.A. Morini, P.C. Schulz, *Colloid Polym. Sci.* 282 (2004) 1063.
- [19] L. Kong, S. Liu, X. Yan, Q. Li, H. He, *Micropor. Mesopor. Mater.* 81 (2005) 251.
- [20] F. Chen, L. Luang, Q. Li, *Chem. Mater.* 9 (1997) 2685.
- [21] T. Vrålstad, G. Øye, M. Rønning, W.R. Glomm, M. Stöcker, J. Sjöblom, *Micropor. Mesopor. Mater.* 80 (2005) 291.
- [22] J.-M. Rueff, PhD Thesis, Université Louis Pasteur, Strasbourg, France, 2000.
- [23] J.-M. Vincent, A. Skoulios, *Acta Cryst.* 20 (1966) 432.
- [24] J.-M. Rueff, N. Masciocchi, P. Rabu, A. Sironi, A. Skoulios, *Chem. Eur. J.* 8 (2002) 1813.
- [25] A.C. Voegtlin, A. Matijasic, J. Patarin, C. Sauerland, Y. Grillet, L. Huve, *Micropor. Mater.* 10 (1997) 137.
- [26] S. Brunauer, P.H. Emmett, E. Teller, *J. Am. Chem. Soc.* 60 (1938) 309.
- [27] E.P. Barrett, L.G. Joyner, P.P. Halenda, *J. Am. Chem. Soc.* 73 (1951) 373.
- [28] J.H. De Boer, in: D.H. Everett, F.S. Stone (Eds.), *The Structure and Properties of Porous Materials*, Butterworths, London, 1958.
- [29] M. Casu, F. Cesare Marincola, A. Lai, A. Musinu, G. Piccaluga, *J. Non-Cryst. Solids* 232–234 (1998) 329.
- [30] A.B.P. Lever, *Inorganic Electronic Spectroscopy*, second ed., Elsevier, Amsterdam, 1984.
- [31] S.I. Aizawa, S. Funahashi, *Inorg. Chem.* 41 (2002) 4555.
- [32] F.E. Mabbs, D.J. Machin, *Magnetism and Transition Metal Complexes*, Chapman & Hall Ltd., London, 1973.
- [33] R.L. Carlin, *Magnetochemistry*, Springer-Verlag, Berlin, Heidelberg, 1986.
- [34] I.S. Hagemann, P.G. Khalifah, A.P. Ramirez, R.J. Cava, *Phys. Rev. B* 62 (2000) R771.
- [35] P.N. Lisboa-Filho, M.R.C. de Almeida, P.L. Gallo, E. Azevedo, C.A. Paskocimas, E. Longo, W.A. Ortiz, *J. Non-Cryst. Solids* 273 (2000) 277.
- [36] D. Ciuparu, P. Haider, M. Fernández-García, Y. Chen, S. Lim, G.L. Haller, L. Pfefferle, *J. Phys. Chem. B* 109 (2005) 16332.
- [37] T. Vrålstad, W.R. Glomm, M. Rønning, H. Dathe, A. Jentys, J.A. Lercher, G. Øye, M. Stöcker, J. Sjöblom, *J. Phys. Chem. B* 110 (2006) 5386.
- [38] G. Clavel, Y. Guari, J. Larionova, C. Guerin, *New J. Chem.* 29 (2005) 275.